4632 *Macromolecules* **2009**, *42*, 4632–4637
DOI: 10.1021/ma900451e

Macromolecules
ARTICLE

Effect of Molecular Weight and Salt Concentration on Conductivity of Block Copolymer Electrolytes

Ashoutosh Panday,[†,‡] Scott Mullin,[†,‡] Enrique D. Gomez,[‡,§] Nisita Wanakule,[‡] Vincent L. Chen,[‡] Alexander Hexemer,[∥] John Pople,[⊥] and Nitash P. Balsara*[,†,‡,§]

[†]*Environmental Energy and Technologies Division, Lawrence Berkeley National Laboratory, Berkeley, California 94720,* [‡]*Department of Chemical Engineering, University of California, Berkeley, California 94720,* [§]*Materials Sciences Division, Lawrence Berkeley National Laboratory, Berkeley, California 94720,* [∥]*Advanced Light Source (ALS), Lawrence Berkeley National Laboratory, Berkeley, California 94720, and* [⊥]*Stanford Synchrotron Radiation Laboratory (SSRL), Stanford University, Stanford, California 94305*

Received February 27, 2009; Revised Manuscript Received May 4, 2009

ABSTRACT: The ionic conductivity, σ, of mixtures of nearly symmetric polystyrene-*block*-poly(ethylene oxide) copolymers and Li[$N(SO_2CF_3)_2$] (LiTFSI) salt was measured as a function of molecular weight, salt concentration, and temperature. The molecular weight of the poly(ethylene oxide) block, M_{PEO}, was varied from 7 to 98 kg/mol. The molar ratio of lithium to ethylene oxide, r, was varied from 0.02 to 0.10. In general, σ increases with increasing M_{PEO} for all values of r. The data can be summarized by plots of normalized conductivity, σ_n, versus M_{PEO}, where $\sigma_n = \sigma/(f\phi_{PEO}\sigma_{PEO})$, ϕ_{PEO} is the PEO volume fraction in the copolymer, σ_{PEO} is the conductivity of PEO homopolymer, and f is a morphology-dependent factor set equal to 2/3 for our lamellar samples. The temperature-dependent conductivity data at a given salt concentration collapse onto a single curve when plotted in this format. At $r = 0.085$, σ_n values reach a plateau in the vicinity of unity in the high M_{PEO} limit. At other values of r, σ_n continues to increase with M_{PEO} within the experimental range and reaches a value of around 0.5 in the high M_{PEO} limit.

Introduction

Flammable organic liquid electrolytes are ubiquitous in current lithium batteries. Replacing the liquid by a solid electrolyte has been a long-standing goal of the battery industry due to the promise of better safety and the potential to produce batteries with higher energy densities. The latter may be accomplished by replacing the conventional graphite electrode by a lithium foil. Around 1990, several industrial and academic research groups[1−19] were formed to enable commercialization of all-solid rechargeable lithium metal batteries. The dry electrolyte that featured prominently in this research was a mixture of homopolymer poly(ethylene oxide) (PEO) and lithium salts. In spite of reasonable conductivities, efforts to build lithium metal polymer batteries did not bear fruit. An important failure mechanism of these batteries was the growth of lithium dendrites from the anode surface during charging.[20−24] Models by Newman[25−27] predicted that dendrite growth could be prevented if the shear modulus, G, of the solid electrolye exceeded a certain critical value which was orders of magnitude above that of PEO. The development of solid electrolytes with high ionic conductivity and high shear modulus is, however, a nontrivial task due to the coupling between ion and momentum transport. High ionic conductivity is obtained in soft polymers such as PEO where rapid segmental motion, which is needed for ion transport,[17,18] necessarily results in a decrease in the rigidity of the polymer.[19] It is worth noting in this context that the shear modulus of liquids is identically zero. Thus, dendrite growth in lithium−metal batteries cannot be stopped by conventional liquid electrolytes.

We propose that the mechanical and electrical properties of dry polymer electrolytes can be decoupled by using block copolymers with cocontinuous microphases wherein one of the microphases conducts ions and is thus necessarily soft, while the other is a hard insulator. In ref 28, which contains a comprehensive summary of prior work on the conductivity of block copolymer electrolytes, it was demonstrated that the ionic conductivity of mixtures of symmetric polystyrene-*block*-poly(ethylene oxide) (SEO) copolymers and a lithium salt Li[$N(SO_2CF_3)_2$] (LiTFSI) increases with increasing molecular weight of the PEO block, M_{PEO}. It is well-known that the stiffness of all polymers, homopolymers as well as block copolymers, increases with increasing molecular weight. The use of high molecular weight copolymers thus enables optimization of both ionic conductivity and mechanical properties of the electrolyte. This conclusion is very different from previous studies of nanostructured polymer electrolytes.[7,8,29−43] For example, Mayes and co-workers[39−41] studied a series of graft−block copolymers and reported that ionic conductivity is enhanced when a conducting block is attached to a soft rubbery block rather than a hard glassy block. The effect of molecular weight of the copolymers on conductivity was not considered in refs 39−41.

The work in ref 28 was restricted to relatively low salt concentration. The molar ratio of Li to ethylene oxide, r, was held fixed at 0.02. In the case of homopolymers, ionic conductivity is a nonmonotonic function of r.[44] At low values of r, ionic conductivity increases with increasing r due to the increase in the concentration of ionic species. At high values of r, ionic conductivity decreases with increasing r due to ion pairing and physical cross-linking[45] resulting from coordination between Li^+ and polymer chains. The peak in the conductivity of symmetric SEO copolymers occurs when r is in the vicinity of 0.1. Consequently, the conductivity of SEO copolymers at $r = 0.02$ ranged between 1×10^{-4} and 7×10^{-4} S/cm, a value that is too low for commercial battery applications. Our objective is to

*To whom correspondence should be addressed.

 Published on Web 06/05/2009

Table 1. Characteristics of the SEO($a-b$) Block Copolymers Used in This Study

name	M_{PS} (kg/mol)	M_{PEO} (kg/mol)	PEO volume fraction, ϕ_{PEO}	PEO weight fraction	PDI	morphology	normalized expansion coefficient, m[b]
PEO		20	1	1			
SEO(6−7)	6	7	0.52	0.53	1.02	lamellae	2.8
SEO(16−16)	16	16	0.48	0.50	1.09	lamellae	2.0
SEO(36−24)	36	24	0.38	0.40	1.10	HPL[a]	1.6
SEO(37−25)	37	25	0.39	0.41	1.04	lamellae	1.4
SEO(40−31)	40	31	0.42	0.44	1.12	HPL[a]	2.1
SEO(40−54)	40	54	0.55	0.58	1.20	lamellae	2.2
SEO(53−68)	53	68	0.54	0.56	1.05	lamellae	2.8
SEO(74−98)	74	98	0.55	0.57	1.14	lamellae	1.3

[a] Hexagonally perforated lamellae. [b] Normalized expansion coefficient, m, is obtained by least-squares linear fits of d/d_0 vs r data ($d/d_0 = 1 + mr$), where r is [Li]/[EO], d is the periodicity of the ordered salt-containing block copolymer, and d_0 is that of the neat copolymer sample with $r = 0$.

see if the observed increase in conductivity with molecular weight holds for higher values of r, i.e., for samples with higher conductivities. We note in passing that all other studies of dry polymer electrolytes have concluded that increasing molecular weight leads to a decrease in ionic conductivity.[46,47] In the case of PEO/$LiSO_2CF_3$ mixtures, the ionic conductivity decreases[46] with increasing molecular weight (M) for M values lower than the entanglement threshold (about 1 kg/mol) and is independent of M when M is greater than 1 kg/mol. In contrast, the conductivity of symmetric SEO copolymers continues to increase with molecular weight even when M_{PEO} is as high as 98 kg/mol.

The introduction of a nonconducting microphase will undoubtedly decrease the overall conductivity of the block copolymer relative to that of the ionically conducting homopolymer. The factors governing this decrease are (1) the morphologies of the conducting and nonconducting microphases, (2) the orientation of the conducting domains relative to the electrodes, (3) the connection between the conducting domains at grain boundaries and other defects, and (4) the morphology of the interface between the block copolymer and the electrode. If, for example, the nonconducting block forms a wetting layer at the electrode or the orientation of an anisotropic microphase such as lamellae or cylinders is parallel to the electrodes, then the measured conductivity of the block copolymer will be much lower than that of the homopolymer. On the other hand, if the conducting channels are oriented perpendicular to the electrodes, then the expected conductivity of the block copolymer at corresponding temperature, $\sigma_{perp}(T)$, will be given by

$$\sigma_{perp}(T) = \phi_{PEO}\sigma_{PEO}(T) \quad (1)$$

where ϕ_{PEO} is the volume fraction of the PEO microphase in the block copolymer and $\sigma_{PEO}(T)$ is the conductivity of the PEO homopolymer at the temperature of interest. Here we assume that the intrinsic conductivity of the PEO microphase in a block copolymer is identical to that of the PEO homopolymer and that the molecular weights of the PEO chains are above the entanglement threshold. Within the present framework, $\sigma_{perp}(T)$ represents the maximum possible conductivity of block copolymer electrolytes.

On the basis of simple models of diffusion,[48] it can be argued that the conductivity of a block copolymer sample composed of randomly oriented lamellae grains (our case) would be given by

$$\sigma_{random}(T) = (2/3)\sigma_{perp}(T) \quad (2)$$

because, on average, one-third of the conductive pathways would be oriented parallel to the electrodes, and these pathways will not contribute to ion transport between electrodes. One could view the (2/3) factor in eq 2 as a morphology-related factor, f. For randomly oriented grains with cylinders of PEO in a nonconducting matrix, $f = 1/3$. We can rewrite eq 2 in a general form as

$$\sigma_{random}(T) = f\sigma_{perp}(T) \quad (3)$$

where f depends on both the microstructure and alignment.

We use $\sigma(T)$ to refer to the measured conductivity of our samples and define a normalized conductivity, $\sigma_n(T)$, as

$$\sigma_n(T) = \sigma(T)/[f\phi_{PEO}\sigma_{PEO}(T)] \quad (4)$$

As indicated in eq 4, the temperature dependence of the normalized conductivity arises from the temperature dependence of $\sigma(T)$ and $\sigma_{PEO}(T)$. The main goal of this paper is to report on the effect of M_{PEO} and r on $\sigma(T)$ and $\sigma_n(T)$.

Experimental Section

Polystyrene-*block*-poly(ethylene oxide) copolymers were synthesized by sequential anionic polymerization of styrene followed by ethylene oxide using methods described in refs 49 and 50. Prior to the polymerization of the ethylene oxide block, an aliquot of the reaction mixture was isolated and the living chains were terminated to enable characterization of the polystyrene block. The polymers were purified by filtration and precipitation and isolated by freeze-drying. The number-averaged molecular weight (M_n) and the polydispersity index (PDI) of the PS block were obtained by gel permeation chromatography (GPC) comprising a Waters 2690 separations module and a Viscotek triple detector system calibrated for polystyrene standards. The PDIs of the PS blocks were less than or equal to 1.10. The volume fraction of each block was determined using ^{1}H nuclear magnetic resonance (NMR) spectroscopy. The PDI of the SEO copolymers, based on GPC using polystyrene standards, was less than 1.20. The copolymers are labeled SEO($a-b$), where a and b are the number-averaged molecular weights of the PS and PEO blocks, respectively, in kg/mol. A poly(ethylene oxide) homopolymer (PEO) purchased from Fluka was used to measure the temperature dependence of σ_{PEO} in eq 4. The characteristics of the homopolymer and block copolymers used in this study are listed in Table 1.

Polymer electrolytes were prepared by mixing the SEO copolymers with Li[$N(SO_2CF_3)_2$] (lithium bis(trifluoromethanesulphonyl)imide, LiTFSI) salt in an MBraun glovebox, maintaining an argon atmosphere with ultralow concentrations of water, oxygen, and organic solvents. The levels of H_2O and O_2 were less than 0.1 and 2 ppm, respectively, and organic solvent concentration was below 10 ppm. Approximately 0.3 g of SEO samples was placed in glass vials, vacuum-dried at 90 °C for a minimum of 24 h in the antechamber of the glovebox, and transferred directly into the glovebox. The LiTFSI salt (Aldrich, as received) was separately vacuum-dried at 160 °C in the antechamber of glovebox and then transferred directly into the glovebox. The dried SEO copolymer samples were dissolved in

20 mL of dry benzene using a temperature-controlled hot plate at 45 °C for 3 days. In a separate vial, a 10:1 w/w THF/LiTFSI mixture was prepared by dissolution at room temperature for at least 24 h. The THF used for this study was distilled over calcium hydride (CaH_2). Predetermined amounts of the THF/LiTFSI and SEO/benzene mixtures were then mixed and heated at 45 °C for 3 days to obtain solutions containing the SEO($a-b$)/LiTFSI block copolymer electrolyte sample at the desired value of r. The expected error in r, due to limited accuracy of our balances, is about 3%. The solutions were then transferred into an airtight desiccator which was subsequently connected to a freeze-drying apparatus. To ensure complete solvent removal, the polymer electrolyte mixture was freeze-dried for at least 1 week and then returned to the glovebox for electrochemical characterization.

The fluffy freeze-dried block copolymer electrolyte was hand-pressed into a pellet and placed at the center of a Garolite spacer with 0.125 mm thickness and a central hole 3.88 mm in diameter inside a Teflon bag. The Teflon bag containing the sample was heated in a hand press to about 100 °C for about 30 min, and a bubble-free ca. 150 μm thick disk was obtained. The sample was placed between two mirror-polished stainless steel electrodes, which were held together by poly(ether ether ketone) screws and heated to about 100 °C in a heated press in the glovebox to ensure good contact between the electrodes and the electrolyte. After determining the final sample thickness, the electrode−sample assembly with the screws was placed in a home-built thermostated conductivity cell connected to a Solartron 1260 frequency response analyzer (FRA) with a Solartron 1296 dielectric interface. The real and imaginary components of the impedance, Z' and Z'', respectively, of the samples were measured using the FRA at 10 °C intervals during heating and cooling scans between 40 and 120 °C. An ac signal ranging from 5 to 100 mV in the frequency range (ω) of 10 Hz−1 MHz was applied to generate the appropriate frequency response. The plateau value in the Bode plot of modulus of the complex impedance, $|Z' + iZ''|$, vs ω was taken as the sample resistance. This value was nearly identical to the semicircle touchdown on the Nyquist $-Z''$ vs Z' plot. We present data at temperatures between 80 and 120 °C where the PEO domains are amorphous.

The morphological characterization of the neat and salt-containing diblock copolymer samples was accomplished by small-angle X-ray scattering (SAXS). The samples for SAXS were first annealed at ~100 °C for at least 4 days and then sealed inside homemade gastight sample holders with Kapton windows. The samples were sealed off from the surrounding atmosphere by a rubber gasket and screw assembly. The entire sample preparation procedure for SAXS was done inside the glovebox. Recognizing that no seal is perfect, the sample holders were taken out of the glovebox a few minutes before actual SAXS data acquisition. The SAXS data were obtained at the Advanced Light Source (ALS) at Lawrence Berkeley National Laboratory, Berkeley, CA, using beamline 7.3.3. Some of the SEO and PEO samples were checked for water contamination after completion of electrochemical characterization and SAXS. The water content of the samples determined by a Karl Fischer titration apparatus located in the glovebox was typically less than 10 ppm.

Results and Discussion

The SAXS profiles from all of the SEO samples were qualitatively similar to those reported in ref 28 and contained at least one scattering peak. The domain spacing, d, was taken to be $2\pi/q_{max}$, where q_{max} is the magnitude of the SAXS scattering vector at the primary scattering peak. In Figure 1a, we show the dependence of d on salt concentration, r = [Li]/[EO], at 120 °C for each of the SEO samples. Because of the limited access to the SAXS instrument, most of the samples were only run once. In a few cases, 2−4 separate samples were studied to obtain robust estimates of d. The error bars on some of the data points in Figure 1a indicate the observed standard deviation of such

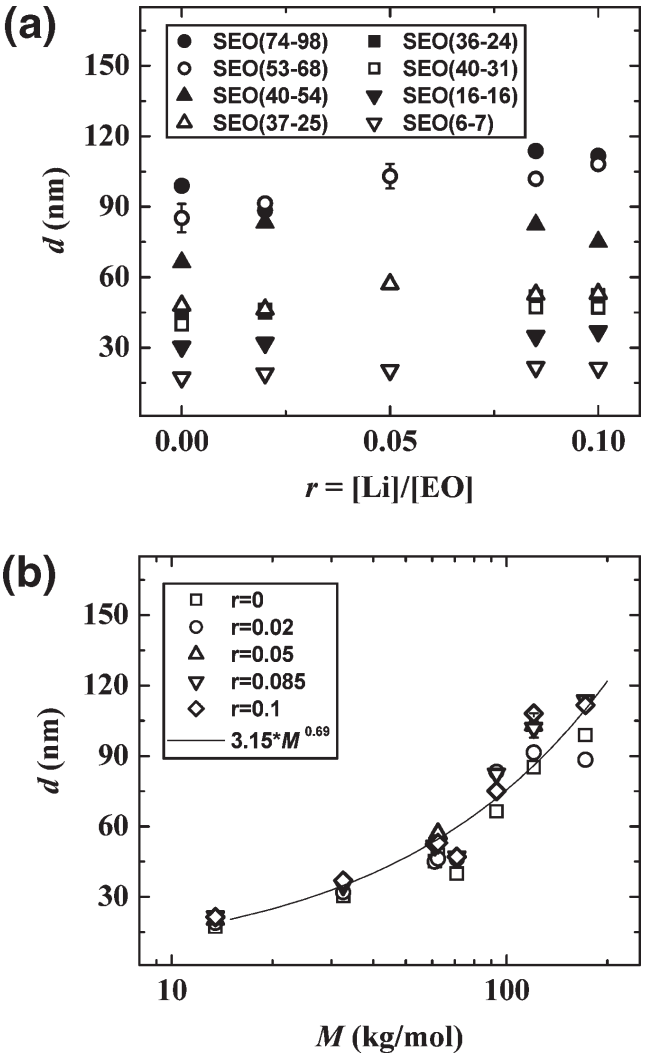

Figure 1. Domain spacing of block copolymer electrolytes at 120 °C as a function of (a) salt concentration, r, the molar ratio of Li to ethylene oxide, and (b) total molecular weight of the SEO copolymers, M. The curve in (b) represents the least-squares power law fit through the data.

repeated measurements. The value of d varies from 114 nm for the highest molecular weight polymer SEO(74−98) to 17 nm for the lowest molecular weight polymer SEO(6−7). Our experiments thus cover a wide range of microdomain sizes. The domain spacing d generally increases with increasing r. Least-squares linear fits of d/d_0 vs r data (where d_0 is the value of d at $r = 0$) were used to quantify the dependence of d on r, $d/d_0 = 1 + mr$. The values of m, which can be interpreted as a normalized expansion coefficient of lamellae due to the addition of salt, obtained at 120 °C are tabulated in Table 1. The fitted values of m range from 1.3 to 2.8. The positive values of m suggest that the addition of LiTFSI increases the effective segregation between PS and PEO domains. The nonmonotonic dependence of m on copolymer molecular weight (see Table 1) indicates that other factors may influence the dependence of d on r. We note in passing that the sensitivity of d on r in our samples is significantly less than that reported in ref 30 for the case of PEO-containing triblock copolymers with $LiClO_4$. It is also evident from Figure 1a that at any given salt concentration d increases with increasing total molecular weight of the copolymer, M. The scaling of d with M for all the samples is shown in Figure 1b. The curve through the data is a least-squares power law fit assuming that $d \sim M^{\nu}$. The experimental value of ν is 0.69 ± 0.03, which is identical to that

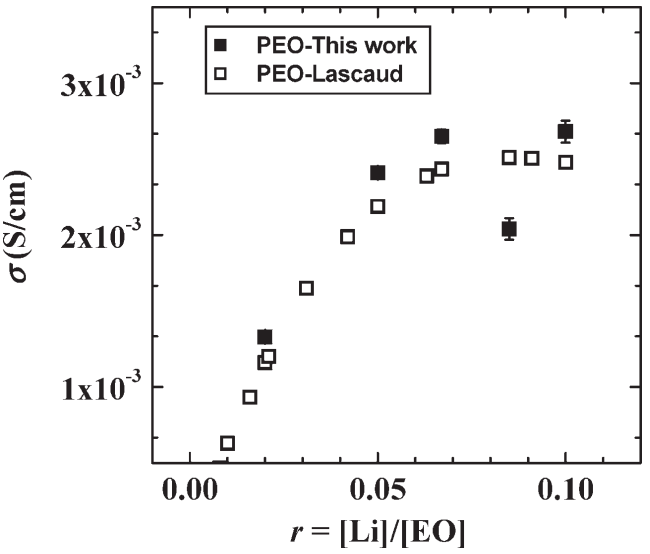

Figure 2. Ionic conductivity of PEO homopolymer vs r, the molar ratio of Li to ethylene oxide at 100 °C obtained in the present study (filled symbols) and taken from the published work of Lascaud et al.[44] (open symbols).

expected from neat diblock copolymers in the strong segregation limit.[51,52]

The morphology of the SEO samples in the neat state was determined by a combination of SAXS and transmission electron microscopy (TEM) as described in ref 28 (not repeated here for brevity), and the results are given in Table 1. We did not attempt TEM on the salt-containing samples due to the lack of equipment necessary to create thin sections in a water-free atmosphere.

In Figure 2 we show the dependence of the conductivity of PEO on salt concentration, r, at 100 °C. Our measurements of $\sigma_{PEO}(T)$ (filled squares) compared reasonably well with those of Lascaud et al.[44] (unfilled squares). The largest deviation between the two data sets is 5×10^{-4} S/cm seen at $r = 0.085$ (Figure 2). We offer no explanation for this difference. We do, however, show explicitly that this deviation does not affect any of the major conclusions of the present study.

In Figure 3a we plot $\sigma(T)$ vs M_{PEO} for the block copolymers in Table 1 at $r = 0.085$ at selected temperatures. For a given value of M_{PEO}, $\sigma(T)$ increases with temperature, in accordance with expectations. We find that $\sigma(T)$ increases monotonically with increasing molecular weight and appears to reach a plateau for $M_{PEO} > 60$ kg/mol. It has been established that ion transport in homopolymers is related to polymer segmental motion. If this were the case for block copolymers, then one expects $\sigma(T)$ to be independent of M_{PEO} in the high molecular weight limit. The data in Figure 3a are consistent with this expectation. However, one expects properties that are dependent on segmental motion of polymers to reach molecular-weight-independent plateaus at molecular weights that are significantly lower than 60 kg/mol. The ionic conductivity of PEO homopolymers reaches a plateau at about 1 kg/mol as do other properties such as the glass transition temperatures of polymers.[46,47,53,54] The large value of polymer molecular weights needed to attain the plateau in Figure 3a and the fact that the conductivity increases with molecular weight indicates that there is a fundamental difference in the mechanism of ion transport in homopolymers and block copolymers. We suggest that chain stretching, a well-established effect in block copolymer microphases, is responsible for this difference.[55]

In Figure 3b we show the dependence of $\sigma_n(T)$ on M_{PEO} for the data set in Figure 3a ($r = 0.085$) using our measured values for the temperature dependence of $\sigma_{PEO}(T)$ for normalization

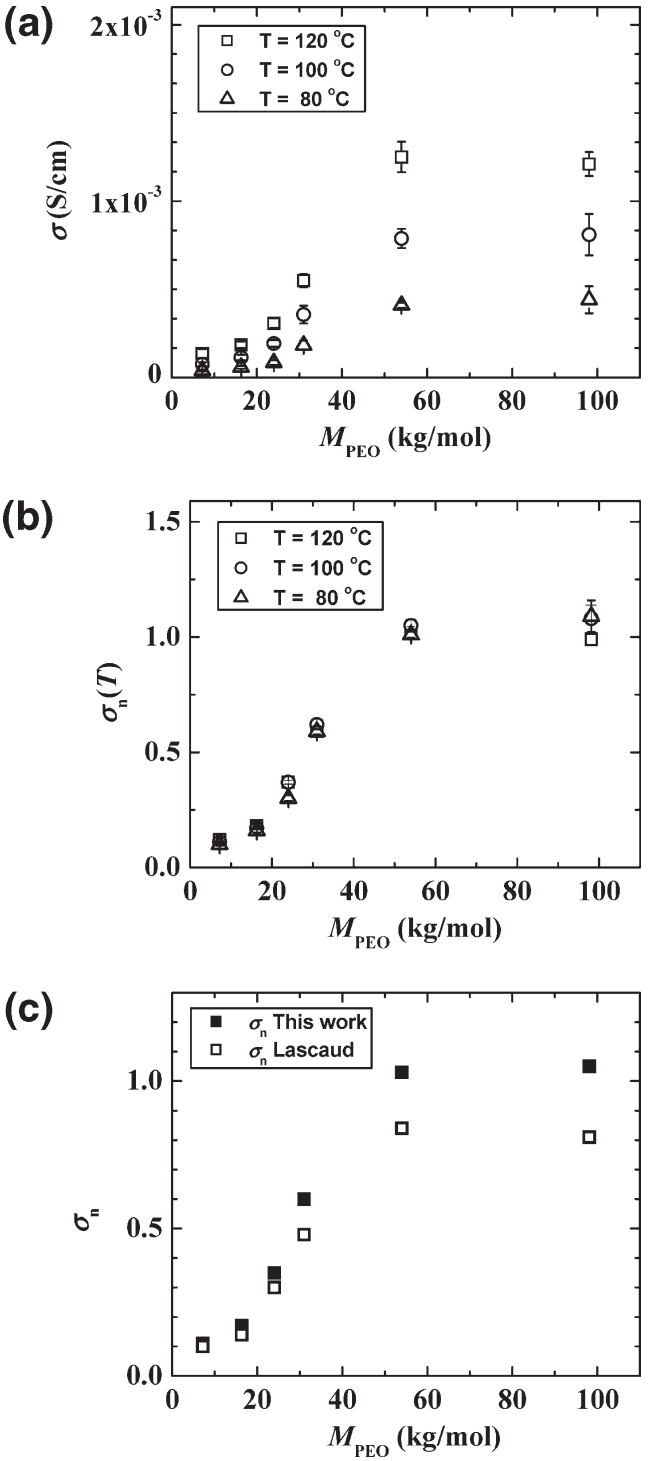

Figure 3. Conductivity of SEO/LiTFSI mixtures with $r = 0.085$ as a function of molecular weight of the PEO block, M_{PEO}, at temperatures of 120, 100, and 80 °C. (a) Ionic conductivity, σ, vs M_{PEO}. (b) Temperature-dependent normalized conductivity, $\sigma_n(T)$, vs M_{PEO} for the data shown in (a) using values of PEO conductivity measured in this study. (c) Temperature-averaged normalized conductivity, σ_n, vs M_{PEO}, for the data shown in (a) using values of PEO conductivity measured in this study (filled squares) and values reported by Lascaud et al.[44] (open squares).

(see eq 4). We use a morphology factor $f = 2/3$ consistently throughout this paper; i.e., we do not distinguish between hexagonally perforated lamellae and ordinary (unperforated) lamellae. We see that all of the data collapse on a universal curve in Figure 3b, indicating that the temperature dependence of $\sigma(T)$

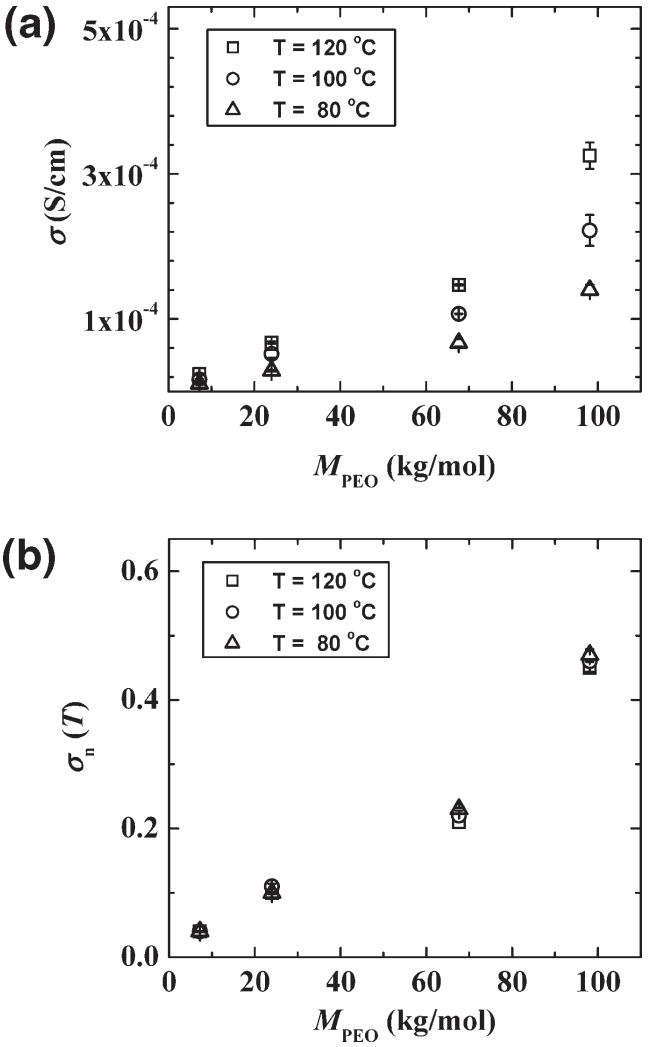

Figure 4. Conductivity of SEO/LiTFSI mixtures with $r = 0.02$ as a function of molecular weight of the PEO block, M_{PEO}, and temperatures of 120, 100, and 80 °C. (a) Ionic conductivity, σ, vs M_{PEO}. (b) Temperature-dependent normalized conductivity, $\sigma_n(T)$, vs M_{PEO} for the data shown in (a) using values of PEO conductivity measured in this study.

obtained from block copolymers is similar to $\sigma_{PEO}(T)$ obtained from PEO homopolymers. This indicates that while the ions in our block copolymers are surrounded by stretched PEO segments, the dynamical properties of the segments that are reflected in the temperature-dependent transport measurements are unaffected by self-assembly.

We define σ_n to be the average value of $\sigma_n(T)$ measured for a given SEO/LiTFSI mixture across our temperature window. In Figure 3c, we show the dependence of σ_n on M_{PEO}. The ordinates of the data in Figure 3c represent averages of the data sets in Figure 3a. The filled symbols in Figure 3c show the dependence of σ_n on M_{PEO} using our measured values of $\sigma_{PEO}(T)$ for normalization. The open symbols show the dependence of σ_n on M_{PEO} using values of $\sigma_{PEO}(T)$ from Lascaud et al.[44] for normalization. It is evident that the qualitative features of the dependence of σ_n on M_{PEO} are not affected by our choice of $\sigma_{PEO}(T)$. The values of σ_n obtained from symmetric SEO samples at $r = 0.085$ are between 0.80 and 1.05 in the high molecular weight limit. In other words, the conductivity of high molecular weight SEO samples with $r = 0.085$ is close to the theoretical limit expected from a collection of randomly oriented but well-connected lamellar grains.[48]

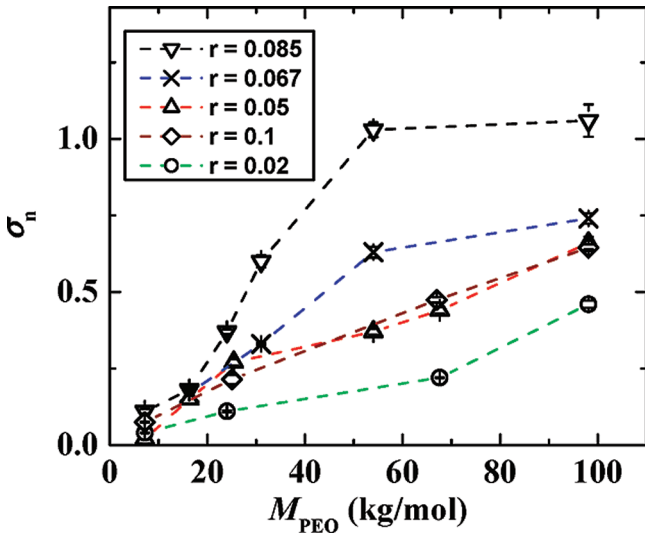

Figure 5. Temperature-averaged normalized conductivity, σ_n, vs M_{PEO} for $r = 0.02-0.10$.

In Figure 4a we plot $\sigma(T)$ vs M_{PEO} at $r = 0.02$. Unlike the $r = 0.085$ data, we do not see a high molecular-weight-independent plateau in these data. Since it is reasonable to expect a molecular-weight-independent plateau for ionic conductivity, we conclude that the molecular weights at which this behavior is obtained at $r = 0.02$ is higher than 100 kg/mol. In Figure 4b we show the dependence of σ_n on M_{PEO} for the data set in Figure 4a ($r = 0.02$) using our measured values for the temperature dependence of $\sigma_{PEO}(T)$ for normalization. For this set (and all others discussed below), there is no discernible difference in the dependence of σ_n on M_{PEO} if the data of Lascaud et al.[44] are used to normalize the conductivity measurements. As was the case with the $r = 0.085$ data, we find a collapse of the conductivity data onto a universal curve. For $r = 0.02$, the value of σ_n at the highest molecular weight is about 0.5, which is significantly lower than the values obtained at $r = 0.085$. It is not clear at this point if σ_n values as high as unity can be achieved in SEO samples with $r = 0.02$.

While the qualitative trends seen in the $r = 0.02$ data shown in Figure 4 are similar to those presented in ref 28, there are quantitative differences. The conductivity values of the SEO samples reported here are about a factor of 2 lower than those reported in Figure 4 of ref 28. We tentatively attribute this difference to plasticization of the polymer electrolytes in our previous experiments because they were conducted in a glovebox where the organic vapor concentration was neither measured nor controlled. One expects the conductivity of samples with low salt concentration to be sensitive to the presence of contaminants.

We measured the dependence of $\sigma(T)$ on M_{PEO} for three other values of r, $r = 0.05$, 0.067, and 0.10. The data obtained from these samples were qualitatively similar to those shown in Figure 4. For each value of r, the $\sigma_n(T)$ vs M_{PEO} data collapsed onto a universal curve. We can thus assert that the dependence of conductivity of SEO samples on M_{PEO}, T, and r can be summarized by σ_n vs M_{PEO} plots, shown in Figure 5. For $r \leq 0.085$, we find that σ_n for a given value of M_{PEO} increases with increasing r. In addition, the dependence of σ_n on M_{PEO} has a sigmoidal character, increasing slowly with molecular weight in the low molecular weight limit and then increasing rapidly with molecular weight at intermediate molecular weights. No evidence of a high molecular weight plateau is seen at $r = 0.02$, 0.05, and 0.10. At $r = 0.067$, we see a hint of a high molecular weight plateau; the ionic conductivity of samples with $M_{PEO} = 54$ and 98 kg/mol are with 15% of each other. It appears that the plateau value of σ_n for

$r = 0.067$ is between 0.7 and 0.8, which is significantly lower than that obtained at $r = 0.085$. The high molecular weight plateau is most clearly seen at $r = 0.085$. Increasing r from 0.085 to 0.10 results in a significant decrease in σ_n at all values of M_{PEO}. The dependence of σ_n on M_{PEO} at $r = 0.10$ and $r = 0.05$ are almost indistinguishable. The smoothness of the dependence of σ_n on M_{PEO} regardless of the morphology (lamellae vs hexagonally perforated lamellae) at all values of r indicates that conductivity is not a strong function of morphology. Typical TEM images of lamellae and perforated lamellae of our samples at $r = 0$ are given in Figure 3 of ref 28.

Our results are limited to a temperature range between 80 and 120 °C where the PEO domains are amorphous. They are thus directly applicable to the design of high-temperature batteries. Further work is needed to see if similar trends hold in copolymers that conduct ions at room temperature.

Conclusions

The ionic conductivity of symmetric SEO block copolymers and LiTFSI mixtures, $\sigma(T)$, was studied as a function of r and M_{PEO}. Regardless of r, we find that $\sigma(T)$ increases with increasing M_{PEO}. The quantitative dependence of $\sigma(T)$ on r and M_{PEO} can be summarized by plots of the normalized conductivity, σ_n, vs M_{PEO} shown in Figure 5. These curves have a sigmoidal shape at all values of r. σ_n reaches a high molecular-weight plateau in the vicinity of unity at $r = 0.085$. We conclude that SEO samples with $r = 0.085$ and M_{PEO} values that exceed 60 kg/mol are optimal for battery electrolyte applications.

Acknowledgment. This work was conducted within the Batteries for Advanced Transportation Technologies (BATT) Program, supported by the U.S. Department of Energy FreedomCAR and Vehicle Technologies Program. Use of the Advanced Light Source at Lawrence Berkeley National Laboratory was supported by the U.S. Department of Energy, Office of Science, Office of Basic Energy Sciences, under Contract DE-AC02-05CH11231. We thank Dr. Hany B. Eitouni, Dr. Mohit Singh, Professor John Newman, Dr. Gao Liu, and Dr. Venkat Srinivasan for helpful discussions.

References and Notes

(1) Armand, M. B.; Chabagno, J. M.; Duclot, M. *Fast Ion Transport in Solids*; Vashista, P., Mundy, J. N., Shenoy, G. K., Eds.; North-Holland: New York, 1979.
(2) Berthier, C.; Gorecki, W.; Minier, M.; Armand, M.; Chabagno, J.-M.; Rigaud, P. *Solid-State Ionics* **1983**, *11*, 91.
(3) Armand, M. *Annu. Rev. Matter Sci.* **1986**, *16*, 245–261.
(4) Armand, M. *Adv. Mater.* **1990**, *2*, 278–286.
(5) Gorecki, W.; Belorizky, E.; Berthier, C.; Donoso, P.; Armand, M. *Electrochim. Acta* **1992**, *37*, 1685–1687.
(6) Wright, P. V. *Br. Polym. J.* **1975**, *7*, 319–327.
(7) Giles, J. R. M.; Gray, F. M.; Maccallum, J. R.; Vincent, C. A. *Polymer* **1987**, *28*, 1977–1981.
(8) Gray, F. M.; Maccallum, J. R.; Vincent, C. A.; Giles, J. R. M. *Macromolecules* **1988**, *21*, 392–397.
(9) Gray, F. M. *Solid Polymer Electrolytes. Fundamentals and Technological Applications*; VCH: Weinheim, 1991.
(10) Robitaille, C. D.; Fauteux, D. *J. Electrochem. Soc.* **1986**, *133*, 315–325.
(11) Ratner, M. A.; Shriver, D. F. *Chem. Rev.* **1988**, *88*, 109–124.
(12) Scrosati, B. *Applications of Electroactive Polymers*; Chapman Hall: London, 1993.
(13) Scrosati, B. *Chem. Rec.* **2001**, *1*, 173–181.
(14) Bouchet, R.; Lascaud, S.; Rosso, M. *J. Electrochem. Soc.* **2003**, *150*, A1385–A1389.
(15) Bruce, P. G.; Gray, F. M.; Shi, J.; Vincent, C. A. *Philos. Mag. A* **1991**, *64*, 1091–1099.
(16) Arbizzani, C.; Mastragostino, M.; Hamaide, T.; Guyot, A. *Electrochim. Acta* **1990**, *35*, 1781–1785.
(17) Watanabe, M.; Sanui, K.; Ogata, N.; Kobayashi, T.; Ohtaki, Z. *J. Appl. Phys.* **1985**, *57*, 123–128.
(18) Kakihana, M.; Schantz, S.; Torell, L. M. *J. Chem. Phys.* **1990**, *92*, 6271–6277.
(19) Boden, N.; Leng, S. A.; Ward, I. M. *Solid State Ionics* **1991**, *45*, 261–270.
(20) Tarascon, J. M.; Armand, M. *Nature (London)* **2001**, *414*, 359–367.
(21) Brissot, C.; Rosso, M.; Chazalviel, J.-N.; Lascaud, S. *J. Power Sources* **1999**, *81−82*, 925–929.
(22) Buriez, O.; Han, Y. B.; Hou, J.; Kerr, J. B.; Qiao, J.; Sloop, S. E.; Tian, M.; Wang, S. *J. Power Sources* **2000**, *89*, 149–155.
(23) Dolle, M.; Sannier, L.; Beaudoin, B.; Trentin, M.; Tarascon, J.-M. *Electrochem. Solid-State Lett.* **2002**, *5*, A286–A289.
(24) Rosso, M.; Gobron, T.; Brissot, C.; Chazalviel, J.-N.; Lascaud, S. *J. Power Sources* **2001**, *97−98*, 804–806.
(25) Monroe, C.; Newman, J. *J. Electrochem. Soc.* **2003**, *150*, A1377–A1384.
(26) Monroe, C.; Newman, J. *J. Electrochem. Soc.* **2004**, *151*, A880–A886.
(27) Monroe, C.; Newman, J. *J. Electrochem. Soc.* **2005**, *152*, A396–A404.
(28) Singh, M.; Odusanya, O.; Wilmes, G. M.; Eitouni, H. B.; Gomez, E. D.; Patel, A. J.; Chen, V. L.; Park, M. J.; Fragouli, P.; Iatrou, H.; Hadjichristidis, N.; Cookson, D.; Balsara, N. P. *Macromolecules* **2007**, *40*, 4578–4585.
(29) Epps, T. H.; Bailey, T. S.; Pham, H. D.; Bates, F. S. *Chem. Mater.* **2002**, *14*, 1706–1714.
(30) Epps, T. H.; Bailey, T. S.; Waletzko, R.; Bates, F. S. *Macromolecules* **2003**, *36*, 2873–2881.
(31) Hirahara, K.; Takano, A.; Yamamoto, M.; Kazama, T.; Isono, Y.; Fujimoto, T.; Watanabe, O. *React. Funct. Polym.* **1998**, *37*, 169–182.
(32) Hoshino, K.; Yoshio, M.; Mukai, T.; Kishimoto, K.; Ohno, H.; Kato, T. *J. Polym. Sci., Part A: Polym. Chem.* **2003**, *41*, 3486–3492.
(33) Huiming, M.; Hillmyer, M. A. *Soft Mater.* **2006**, *2*, 57–59.
(34) Kishimoto, K.; Yoshio, M.; Mukai, T.; Yoshizawa, M.; Ohno, H.; Kato, T. *J. Am. Chem. Soc.* **2003**, *125*, 3196–3197.
(35) Kosonen, H.; Valkama, S.; Hartikainen, J.; Eerikainen, H.; Torkkeli, M.; Jokela, K.; Serimaa, R.; Sundholm, F.; ten Brinke, G.; Ikkala, O. *Macromolecules* **2002**, *35*, 10149–10154.
(36) Niitani, T.; Shimada, M.; Kawamura, K.; Dokko, K.; Rho, Y. H.; Kanamura, K. *Electrochem. Solid-State Lett.* **2005**, *8*, A385–A388.
(37) Niitani, T.; Shimada, M.; Kawamura, K.; Kanamura, K. *J. Power Sources* **2005**, *146*, 386–390.
(38) Ruzette, A.-V. G.; Soo, P. P.; Sadoway, D. R.; Mayes, A. M. *J. Electrochem. Soc.* **2001**, *148*, A537–A543.
(39) Soo, P. P.; Huang, B. Y.; Jang, Y. I.; Chiang, Y. M.; Sadoway, D. R.; Mayes, A. M. *J. Electrochem. Soc.* **1999**, *146*, 32–37.
(40) Trapa, P. E.; Huang, B. Y.; Won, Y. Y.; Sadoway, D. R.; Mayes, A. M. *Electrochem. Solid-State Lett.* **2002**, *5*, A85–A88.
(41) Trapa, P. E.; Won, Y. Y.; Mui, S. C.; Olivetti, E. A.; Huang, B. Y.; Sadoway, D. R.; Mayes, A. M.; Dallek, S. *J. Electrochem. Soc.* **2005**, *152*, A1–A5.
(42) Wang, C. X.; Sakai, T.; Watanabe, O.; Hirahara, K.; Nakanishi, T. *J. Electrochem. Soc.* **2003**, *150*, A1166–A1170.
(43) Yoshio, M.; Mukai, T.; Ohno, H.; Kato, T. *J. Am. Chem. Soc.* **2004**, *126*, 994–995.
(44) Lascaud, S.; Perrier, M.; Vallee, A.; Besner, S.; Prudhomme, J.; Armand, M. *Macromolecules* **1994**, *27*, 7469–7477.
(45) Matsumiya, Y.; Balsara, N. P.; Kerr, J. B.; Inoue, T.; Watanabe, H. *Macromolecules* **2004**, *37*, 544–553.
(46) Shi, J.; Vincent, C. A. *Solid State Ionics* **1993**, *60*, 11–17.
(47) Cheung, I. W.; Chin, K. B.; Greene, E. R.; Smart, M. C.; Abbrent, S.; Greenbaum, S. G.; Prakash, G. K. S.; Surampudi, S. *Electrochim. Acta* **2003**, *48*, 2149–2156.
(48) Sax, J.; Ottino, J. M. *Polym. Eng. Sci.* **1983**, *23*, 165–176.
(49) Hadjichristidis, N.; Iatrou, H.; Pispas, S.; Pitsikalis, M. *J. Polym. Sci., Part A: Polym. Chem.* **2000**, *38*, 3211–3234.
(50) Quirk, R. P.; Kim, J.; Kausch, C.; Chun, M. S. *Polym. Int.* **1996**, *39*, 3–10.
(51) Helfand, E. *Macromolecules* **1975**, *8*, 552–556.
(52) Helfand, E.; Wasserman, Z. R. *Macromolecules* **1976**, *9*, 879–888.
(53) Thomas, G.; Fox, P. J. F. *J. Polym. Sci.* **1954**, *14*, 315–319.
(54) Thomas, G.; Fox, J.; Flory, P. J. *J. Appl. Phys.* **1950**, *21*, 581–591.
(55) Gomez, E. D.; Panday, A.; Feng, E. H.; Chen, V.; Stone, G. M.; Minor, A. M.; Kisielowski, C.; Downing, K. H.; Borodin, O.; Smith, G. D.; Balsara, N. P. *Nano Lett.* **2009**, *9*, 1212–1216.